Satisfaction of Modeling Requirements for Intelligent Navigation Systems: Risk Management Context

Nadhir Mansour Ben Lakhal[1,2(✉)], Othman Nasri[2], Lounis Adouane[3], and Jaleleddine Ben Hadj Slama[2]

[1] Institut Pascal, UCA/SIGMA-UMR CNRS 6602, Clermont Auvergne University, Clermont-Ferrand, France
nadhir_mansour.ben_lakhal@etu.uca.fr

[2] LATIS Lab, National Engineering School of Sousse (ENISo), University of Sousse, BP 264, 1023 Sousse Erriadh, Tunisia

[3] Heudiasyc UMR CNRS/UTC 7253, Université de Technologie de Compiègne, 60203 Compiègne, France
lounis.adouane@hds.utc.fr

Abstract. This work aims to boost the reliability and safety of Intelligent Transportation Systems (ITSs). To meet this goal, a particular risk assessment and management scheme is introduced to provide navigation approaches with strong safety guarantees. On the one hand, the interval analysis is adopted to develop a high fidelity model used for risk assessment purposes. This model is based on a set-membership computation of the Time-To-Collision (TTC) indicator. The TTC approximation methodology, which fits well the car-following scenario, takes into account several uncertainties of distinct sources. Even more, a novel second-order set-membership TTC formalization is introduced by solving a polynomial equation with interval coefficients. This formalization is suggested in an effort to diminish modeling errors. Both the first and second order interval-based TTC are improved via a correlation analysis-based statistical process. On the other hand, the complexity aspects of modern architectures are analyzed in this work. The tackled analysis emphasizes the destructive impacts of the inter/intra-vehicular communication on ITSs reliability. Thus, a Response Time Analysis (RTA) scheme is integrated into the proposed risk management to consider explicitly the communication latency-related material constraints. Then, the RTA results are involved into the simulation work. Finally, the simulation results applied on an adaptive cruise control system of both high/low-order TTC formalizations demonstrate that the low-order model inaccuracy is compensated. Through the interval/correlation analysis and the consideration of the material constraints, a great balance between modeling accuracy and simplicity is performed.

Keywords: Intelligent vehicles · Risk management · Interval-based modeling · Correlation analysis · Communication delays · Time to collision

O. Gusikhin et al. (Eds.): ICINCO 2020, LNEE 793, pp. 456–478, 2022.
https://doi.org/10.1007/978-3-030-92442-3_23

1 Introduction

Risk assessment and management should be inspected carefully to employ Intelligent Transportation Systems (ITSs) in public roads [31]. For the sake of safety, focus is currently given to provide efficient solutions for in-road risk identification. Thus, factors that stand behind the reliability and accuracy of safety verification techniques should be analyzed.

At first, the risk assessment task consists in identifying in real-time the potential in-road hazards through a deep situational awareness of risk. The required awareness about threats is imperatively obtained by analyzing the environmental data. Risks may be directly captured based on several vision systems co-joined with scene analysis methods. The collected images/videos are processed and analyzed to verify/validate the vehicle safety [1]. However, these methods are computationally demanding and not always suitable for real-time safety critical applications. Besides, problems such as shadowing and occlusion may render results of the scene analysis incredible [46]. As an alternative, it is preferable to rely on more simple physical parameters describing vehicle motions, such as inter-vehicle distances, velocities and accelerations, to interpret the risk assigned to a given situation. According to this understanding, the ITS community has focused in introducing various analytical risk indicators, which are calculated through real measurements of the stated parameters. These indicators use physical-based models to make the risk identification closet to reality. In such a way, the risk assessment efficiency is related to these indicators' accuracy.

To overcome uncertainty impacts on the risk indicators, several methods have been proposed in the literature [22,28]. The uncertainty is propagated into the navigation process via stochastic models such as the Kalman filter, etc. A specific probability distribution, as the Gaussian function, is assumed to describe the uncertainty evolution. This assumption is controversial, and changes in noise features may occur [35]. Additionally, most uncertainty evolution models are sensitive to non-linearity [40]. On top of that, an accurate knowledge of the initial states of the studied system is required, which is not evident [32]. Hence, it is important to study alternative approaches that are less sensitive to these errors.

In particular, the Time To Collision (TTC) has been widely used for risk identification [18,19]. Tremendous attempts have been made to improve the precision of the TTC models. A comparative study between diverse TTC formalizations could be found in [17]. A hidden Markov model has been used to predict the driving intention of nearby vehicles for more accurate TTC estimation [44]. Algorithms computing distances between boxes bounding vehicles were proposed to calculate TTC for complex traffic scenarios [40]. A vehicle motion-based concept, named looming, was exploited to decrease the TTC false alarms [41].

Interval analysis is a reliable way to handle uncertainties/modeling imperfections [20]. It turns standard data to intervals to bound uncertainty impacting the studied system [30]. Correspondingly, interval analysis may contribute strongly in characterizing the uncertainty evolution into intelligent transportation systems. In the previous work, an interval-based model to compute TTC

for a car-following scenario was proposed to handle uncertainties [24,25]. A novel second-order interval-based TTC over-approximation was suggested to consider more parameters intervening in the car-following scenario. The high-order model consists in a quadratic polynomial with interval coefficients generated from vehicles' motion equations. Moreover, the first and second interval TTC over-approximation were optimized via a data-driven characterization of correlation that would relate the navigation system variables.

In the previous work [25], it was proved that safety is only guaranteed with the application of risk management solutions strongly aware of the intra/inter-vehicular communication delays. Nonetheless, this previous work did not provide a clear strategy allowing a reliable quantification of such latency. From this scope, we build on the previous work to cope with this issue. Experimental and theoretical-based approaches are introduced in this context. The results of communication latency quantification are involved explicitly in the simulation work, which is undertaken through a model of an Adaptive Cruise Control (ACC). The performances of the interval high and low-order TTC in conducting the risk worst-case analysis are compared. The quality of the set-membership modeling joined with the correlation analysis is evaluated in terms of accuracy and simplicity.

The rest of this paper is arranged as follows: Sect. 2 highlights the need to consider the communication latencies by the risk assessment level through a brief analysis of modern ITS architectures. Section 3 introduces the first and second-order TTC interval-based formalizations. Section 4 presents a complete scheme, which is integrated into the risk management level, to enhance the robustness against the communication delays. Section 5 presents an algorithm to find roots for an interval polynomial to approximate the TTC. Section 6 explains the correlation analysis role in ameliorating the findings of the TTC set-membership models. Section 7 presents the simulation results. Section 8 concludes the results of this work and discusses some future work.

2 Modern ITS Architecture Complexity-Issued Challenges

Indeed, the architecture of modern ITSs depicts boundless proofs of complexity. More importantly, a new wave of technologies, called Advanced Driver-Assistance Systems (ADASs), are currently implemented into such architectures in order to increase the in-road safety and the comfort of drivers. A detailed list of such systems and a brief description of their main tasks are available in Table 1.

Despite their important role in providing more reliable and trustworthy performances of intelligent vehicles, the emergent ADASs have entailed several complications. First of all, these systems have contributed to the appearance of large scale automotive embedded systems [10]. A direct impact related to this fact is data proliferation into in-vehicular systems.

The increase in the number of Electronic Control Units (ECUs) in automotive embedded systems has duplicated rates of the exchanged data between the

Table 1. Different categories of ADASs.

System	Assigned task	Ref
Adaptive Cruise Control (ACC)	-Perform regular control of velocity to ensure driver comfort -Maintain a safety distance from an in-front car	[29]
Enhanced driver visibility system	-Assist driver to overcome day/night-time visibility troubles -Provide warnings about driving zones affected by fog	[33]
Pedestrian recognition system	-Detect road crossing persons and deliver warnings to driver -Anticipate pedestrian behaviors to capture collision risks	[6]
Road sign recognizing	-Enhance driver awareness about road signalization	[37]
Driver distraction detection systems	-Inspect the driver vigilance -Monitor the driver eyes or head movements	[3]
Smart lane departure warning	-Warn driver in case of departure from the driving lanes -Manage position estimation for several road models	[13]
Self-parking/ parking assistance	-Help drivers in finding vacant parking location -Track a smooth path towards a vacant spot	[13]
Co-pilot/autopilot system	-Ensure autonomous driving via human-like vehicle control -Alleviate consequences of drivers' slow reactions to threats	[2]
Blind spot detection	-Object detection in blind spot -Side rear blind spot warning for parking lots	[27]
Anti-lock Braking System (ABS)	-Prohibit wheels from sliding during hard braking -Monitor the contact between wheels and road surface	[39]

different vehicular components. An important question should be then answered: are embedded systems of modern vehicles able to support such huge data flows? Indeed, several studies have proven that extra-load of communication into automotive systems limit their capacities in terms of reactivity to hazardous events [34,47].

The vehicular networks of large scale have emphasized also several timing behavioral imperfection of automotive systems. Since these networks include sub-entities of distinct timing characteristics, synchronizing the communication between these latter ones has become more challenging [43]. Hence, the navigation systems are prone more than ever to enormous communication delays. It is worth mentioning that the ADASs operation is definitely sensitive to delays in regard to the critical safety constraints implied in these systems [5].

The extra-connectivity of modern vehicles to the environment is another element that increased the automotive structure complexity. More sensing tools are needed to ensure more reliable perception. In regard to the electrical nature of sensors, more disturbances and noises propagate from the sensing layer to the rest of the automotive systems [14]. Due to these disturbances, more inter-vehicular communication delays are expected.

In accordance with the above complexity analysis of the modern architecture of navigation systems, the intra/inter-communication latencies are the most crucial material constraints threatening the navigation. Consequently, risk management solutions with great awareness of communication latencies are urgently needed. Hence, risk management solutions that handles in general all sorts of uncertainties and the communication latencies in particular will be proposed in the following.

3 Second Order Set-Membership TTC for Car-Following Scenario

Following a given road participant is among the most carried out automated driving maneuvers. It represents also a fundamental task from the hierarchy of the majority of intelligent navigation processes. According to the recent survey presented in [38], the interest on the car-following developments has a central role in heading towards reliable and fully autonomous navigation approaches.

Actually, handling all sorts of uncertainties especially for the car-following scenario is substantial. Following a vehicle requires to be close enough to this latter. For this reason, important number of road accidents are occurring during a car-following, which emphasizes the need for efficient anti-collision solutions dedicated for this driving context. The follower motions are controlled in order to adapt its velocity to the leader vehicle. In this view, uncertain measurements or error sources related to the complicated composition of modern navigation systems can lead to fatal crashes or undesirable discomfort for passengers during a car-following situation. Correspondingly, the current section inspects how to exploit models to make the car-following situation entirely safe.

For a car-following scenario, the TTC is often approximated by the ratio between the distance separating two vehicles and their relative velocity. Instead, the evolution of the spacing distance between the follower and the leader is used in this paper to perform more accurate collision prediction. In this way, all the interactions between vehicles are taken into account. Let consider two vehicles i and j, which are respectively the leader and the follower. V_i, V_j, p_i and p_j are their respective velocities and vector positions. According to [41], the separation evolution between both vehicles is described at each instant by:

– The separation distance [25]:

$$d_{ij} = \sqrt{(p_i - p_j)^T (p_i - p_j)} \tag{1}$$

– The change rate in the separation distance [25]:

$$\dot{d}_{ij} = \frac{1}{d_{ij}} (p_i - p_j)^T (V_i - V_j) \tag{2}$$

– The variation of the change rate in the separation distance is governed by the following equation [25]:

$$\ddot{d}_{ij} = \frac{1}{d_{ij}}(V_i - V_j)^T(V_i - V_j) - \dot{d}_{ij}^2 \tag{3}$$

Equations (2) and (3) are obtained by the consecutive differentiation of Eq. (1). In practice, d_{ij} is measured in run-time thanks to diverse vehicular tools as a LiDAR or laser scanner. Therefore, the authors in [41] defined TTC_1 as a first order TTC [25]:

$$TTC_1 = -\frac{d_{ij}}{\dot{d}_{ij}} \tag{4}$$

However, Eq. (4) neglects parameter $\ddot{d}_{ij}$. Model simplification is the main source of errors [21]. In an effort to improve accuracy, the authors in [41] upgraded the TTC approximation to a second-order expression. When $\ddot{d}_{ij} \neq 0$, a second-order TTC, denoted TTC_2, is obtained by solving the following polynomial [25]:

$$d_{ij} + \dot{d}_{ij}TTC_2 + \frac{1}{2}\ddot{d}_{ij}TTC_2^2 = 0 \tag{5}$$

Note that Eq. (5) is derived from the vehicles' motion equations. The polynomial roots underline at which instants the two vehicles collide, and the separation between them is zero. Accordingly, the authors in [41] defined the TTC_2 value depending on the roots of Eq. (5). When $\ddot{d}_{ij} = 0$ or the polynomial has no real roots, the low-order model is used and $TTC_2 = TTC_1$. In the case of two real positive roots, the lower value is attributed to TTC_2 since it presents the first collision time. If one of the roots is positive and the other is negative, the positive one is taken. Both roots can be also negative. In such a situation, the root with the closest absolute value to zero is selected because it consists of the most recent interaction between the motions of both vehicles.

Despite its accuracy, the high-order TTC is still sensitive to uncertainty and communication latencies. To overcome this issue, interval analysis is adopted in this paper. Data representation is extended to intervals. Mathematical operations $(+, -, *, /)$ and functions $(sin, cos, etc.)$ are extended to handle intervals [20]. Subsequently, the obtained interval-based models provide over-approximations of results that definitely enclose the exact outputs. Henceforth, $[x] = [\underline{x}, \overline{x}]$ is a real interval, where $\underline{x}$ and $\overline{x}$ are its lower and upper bounds. The width of $[x]$ underlines the uncertainty extent. Accordingly, Eqs. (4) and (5) are represented as [25]:

$$[TTC_1] = -\frac{[d_{ij}]}{[\dot{d}_{ij}]} \tag{6}$$

$$[d_{ij}] + [\dot{d}_{ij}][TTC_2] + \frac{1}{2}[\ddot{d}_{ij}][TTC_2]^2 = 0 \tag{7}$$

Since it describes the real behavior, the second-order set-membership TTC is expected to be more accurate than the first-order one. Equation (7) is a quadratic polynomial with perturbed coefficients. Its roots are intervals enclosing the collision exact time. Solving this polynomial is not feasible by standard analytical approaches. A specific interval polynomial solver must be used. Before doing so, a methodological manner to quantify uncertainties attributed to each interval measurement is introduced. The environmental circumstances, where more uncertainties are expected, are examined. At first, the following assumptions, which are based on the confidence intervals of sensors and communication devices, are admitted:

- The localization inaccuracy is assessed via a signal strength indicator that considers the signal attenuation in the navigation zone.
- The accumulated error impacting the separation distance measurement is considered by an uncertainty range of $\pm 1\%$ from the measured d_{ij}.
- The follower speed V_j is assumed to be exact, and no uncertainty is attributed to this parameter.
- The leader speed V_i is assumed to be erroneous with a range of $\pm 0.5\%$ due to measurement imprecision.

Afterwards, several latencies can slow down the automotive system operation and prohibit the quick management of risks. For that reason, it is advisable to consider such latencies by $[TTC]$. In this work, the follower car is expected to receive the V_i value via a Vehicle-to-Vehicle (V2V) communication. Henceforth, latencies impacting the V2V communication are characterized through interval $[T_{V2V}]$. Besides, $[T_L]$ is a constant interval that takes into account latencies due to update time of sensors and the data propagation into the embedded system. The characterization of $[T_{V2V}]$ and $[T_L]$ will be discussed in next section. Henceforth, the TTC set-membership formalization must consider explicitly the aforementioned uncertainty sources [25]:

$$[TTC_1] = -\frac{[d_{ij}]}{[\dot{d}_{ij}]} - [T_{V2V}] - [T_L] \tag{8}$$

$$[TTC_2] = [\Re] - [T_{V2V}] - [T_L] \tag{9}$$

where $[\Re]$ is the polynomial root of Eq. (7). Similar to the deterministic case detailed above (cf. Eq. (5)), $[\Re]$ is the root corresponding to the first collision time. Figure 1 illustrates the main instructions of the proposed uncertainty quantification strategy to over-approximate the first/second order TTC.

4 Quantification of Communication Delays

Because the disrespect of the communication hard deadlines is disastrous, the assessment of the risk management messages responses time is becoming necessary. In accordance with the interval-based handling of uncertainty, the min/max

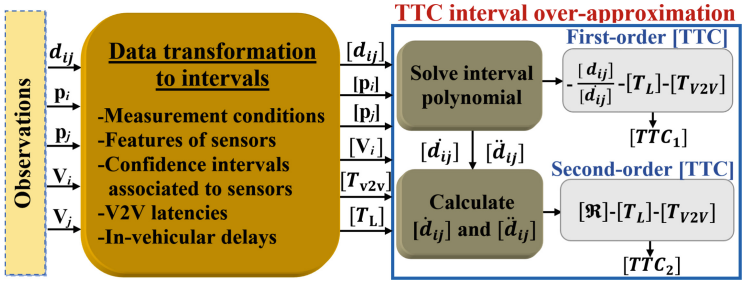

Fig. 1. Interval-based risk management [25].

variation of these delays over time should be properly defined. To meet this purpose, root causes and factors influencing the automotive communication delays should be well-analyzed. Based on the carried analysis, the development of an efficient latency-aware in-road risk management for autonomous navigation can be tackled. In this view, the methodology of how to include the latencies of the V2V communication and respectively the intra-vehicular communication into the risk management-level is detailed below.

4.1 Inter-vehicular Communication Delays

Certainly, making connected vehicles aware about the potential latencies that may occur while communicating with nearby vehicles should permit a more reliable data exchange and inter-vehicular communication. Generally, the existing risk management strategies do not incorporate the communication latency on the risk assessment process. Contrarily to the literature, the proposed safety verification method in this work aims to consider uncertainties invoked by communication delays. Indeed, performances of the communication channel between two connected vehicles depend on the relation ruling the signal strength and vehicles relative location, where one of the vehicles can have a low signal strength or may completely be out of the communication range [8].

Due to the signal interference and disturbances impacting data emission/reception, finding an analytical relation that rules the signal strength and vehicle locations is not evident. Instead, latencies affecting the communication range can be characterized empirically in respect to the velocity of the vehicle broadcasting periodically the required data. At present time, the Dedicated Short-Range Communication (DSRC) and Long-Term Evolution (LTE) technologies are the common wireless technologies that ensure the vehicular connectivity. In this context, the results of a pioneer research work reported in [9] are exploited to quantify the DSRC/LTE delays. The in-field tests carried on in [9] have provided a valuable description of the minimum/maximum variation of these DSRC latencies.

On the one hand, the DSRC and LTE latencies have been characterized relatively to the velocity of the connected vehicle transmitting data. Table 2

presents the empirically recorded latencies affecting the V2V communication for distinct vehicle velocities during real world driving scenarios according to the study depicted in [9].

Table 2. DSRC/LTE delays within different speeds.

Vehicle speed (m/s)	Minimum DSRC latency (ms)	Maximum DSRC latency (ms)	Minimum LTE latency (ms)	Maximum LTE latency (ms)
9	89.35	89.39	1304.85	1305.08
15	93.35	93.84	1319.76	1320.21
22	96.10	96.16	1374.75	1375.43
31	101.47	101.54	1402.30	1402.87

On the other hand, the presence of additional connected vehicles in a same navigation area raises the communication density. When numerous vehicles transmit messages simultaneously, the communication conflicts occurring to reply to data transfer requests provoke supplementary latencies. Thus, for more reliable characterization of the min/max bounds of the DSRC and LTE technologies delays, the experimental study conducted in [9] has also quantified latencies issued from the increasing number of connected vehicles present in the close proximity of the communication range. In this sense, Table 3 depicts bounds of the DSRC/LTE communication delays in function of the number of nearby connected vehicles.

Table 3. DSRC/LTE delays within distinct number of vicinity vehicles.

Neighborhood vehicles number	Minimum DSRC latency (ms)	Maximum DSRC latency (ms)	Minimum LTE latency (ms)	Maximum LTE latency (ms)
10	35.47	35.54	1204.87	1205.23
20	50.66	50.70	1349.39	1350.62
30	66.63	66.66	1742.11	1485.64

Correspondingly, to properly define $[T_{V2V}]$, both the vehicle speed and the number of nearby-connected cars are checked at each sample time to derive the appropriate experimental min/max delays corresponding to these factors.

4.2 In-vehicular Communication Delays

Technically speaking, the characterization of the in-vehicular latency is feasible through a set of commercial software tools. Nevertheless, the use of such tools is expensive, time-consuming and requires a large expertise in the design of in-vehicular embedded systems. As a simple and efficient solution, this work has recourse to the Responses Time Analysis (RTA) to quantify in-vehicular delays. By definition, RTA consists of a theoretically-derived models which estimates the end-to-end transmission time through embedded systems. Usually employed

to validate embedded systems in an early design phase, the RTA concept is used in this work as a deterministic manner to quantify in-vehicular latencies under a risk management context. Indeed, the RTA approach adopted in this work takes into account three main components:

- **Message Maximum Transmission Time:** It underlines the largest period of time needed to broadcast a single frame from a given in-vehicular message. For each in-vehicular communication protocol there is a validated model to assess the temporal marge of delays. For instance, the Controller Area Network (CAN) and FlexRay are the most whispered communication protocols in the automotive field [31]. Correspondingly, Eq. (10) represents the RTA model to compute the maximum transmission time for a CAN message (a 11 bits ID frame) [31]:

$$C^{message} = (55 + 10 \times lm^{CAN}) \times \tau_{bit}^{CAN} \tag{10}$$

  Respectively, the calculation of the maximum transmission time associated to a FlexRay message (a static frame) is given by Eq. (11) [26]:

$$C^{message} = (88 + 10 \times lm^{FR})\tau_{bit}^{FR} \tag{11}$$

  Where lm^{CAN} and lm^{FR} are respectively the number of data bytes incorporated in a CAN and FlexRay messages. Similarly, τ_{bit}^{CAN} and τ_{bit}^{FR} are the required amounts of time to transfer a unique bit of CAN and respectively FlexRay messages. τ_{bit}^{CAN} and τ_{bit}^{FR} are generally fixed according to the communication middleware baudrate and speed.
- **Local Response Times:** In opposite to the existing models in the literature, the applied RTA algorithm conducts a local component analysis. It means that not only the in-vehicular message response time is considered, but also the execution times of the message transmitter/recipient tasks are included into the process of delay evaluation. In such a manner, a comprehensive coverage of the end-to-end transmission time of data is undertaken. Note that in the case of a message exchange between sensors and a given task, the sensor up-date time is assumed as the local response time of the sensing layer.
- **Interference Delays:** The in-vehicular communication is in reality arranged by a priority predefined schedule drawn by the automotive system designers. On the one hand, every message may wait for the communication middleware availability until the end of the broadcast of other higher priority messages. On the other hand, interference delays may take a place in the case where the communication middleware is unavailable due to an already launched transmission of a lower priority message. Readers are referred to [31] for more details about the computation of the interference delays.

Hence, a deterministic evaluation of the end-to-end transmission time of data through the on-bord vehicular communication systems may be realized by simply summing results of the three aforementioned RTA components.

5 Solving Quadratic Interval Polynomial

Finding roots for interval polynomials has been widely discussed in the literature. Several numerical branch and bound algorithms were introduced for this aim [11]. Despite their accuracy, the calculation time of these approaches was unpredictable. One more category of approaches used polynomial factorization and cumbersome mathematical calculation as an inverting interval matrix [45]. Other fast methods were developed [12]. Nevertheless, these approaches provided just a prior estimate for the space containing the real roots. In this work, real roots with sharp bounds of interval polynomials are obtained by studying the interval polynomial boundary functions.

Let consider a quadratic polynomial with the following shape [25]:

$$P([x]) = [a]x^2 + [b]x + [c] \tag{12}$$

Intuitively, $P([x])$ can be expressed within its boundary functions, where: $P([x]) = [\underline{P}([x]), \overline{P}([x])]$. For such a polynomial, $\underline{P}([x])$ and $\overline{P}([x])$ may be derived through all possible combinations between the coefficient bounds. Indeed, eight real single-valued polynomials are given from these combinations [25]:

$$\begin{cases} f_1 = \underline{a}x^2 + \underline{b}x + \underline{c}; & f_2 = \underline{a}x^2 + \underline{b}x + \overline{c} \\ f_3 = \underline{a}x^2 + \overline{b}x + \underline{c}; & f_4 = \underline{a}x^2 + \overline{b}x + \overline{c} \\ f_5 = \overline{a}x^2 + \underline{b}x + \underline{c}; & f_6 = \overline{a}x^2 + \underline{b}x + \overline{c} \\ f_7 = \overline{a}x^2 + \overline{b}x + \underline{c}; & f_8 = \overline{a}x^2 + \overline{b}x + \overline{c} \end{cases} \tag{13}$$

By interpreting the dominant term of $P([x])$, it is evident that $\underline{P}([x])$ and $\overline{P}([x])$ are respectively enclosed between (f_1, f_2, f_3, f_4) and (f_5, f_6, f_7, f_8). It is clear also that [25]:

$$\begin{cases} f_1 \leq f_2; & f_3 \leq f_4 \\ f_6 \geq f_5; & f_7 \geq f_8 \end{cases} \tag{14}$$

Subsequently, we can figure out that [25]:

$$\underline{P(x)} = \begin{cases} P_1 = \underline{a}x^2 + \underline{b}x + \underline{c}, & \text{if } x \geq 0 \\ P_2 = \underline{a}x^2 + \overline{b}x + \underline{c}, & \text{if } x \leq 0 \end{cases} \tag{15}$$

and

$$\overline{P(x)} = \begin{cases} P_3 = \overline{a}x^2 + \overline{b}x + \overline{c}, & \text{if } x \geq 0 \\ P_4 = \overline{a}x^2 + \underline{b}x + \overline{c}, & \text{if } x \leq 0 \end{cases} \tag{16}$$

Note that $P_{i=1..4} = (P_1, P_2, P_3, P_4)$ represents non-interval real boundary functions associated to $P([x])$. To illustrate such a notion, Fig. 2 presents two examples of quadratic polynomials with perturbed coefficients.

An efficient way to find polynomial roots is to determine sets where: $\underline{P}([x]) \leq 0 \leq \overline{P}([x])$. Eventually, estimating sharp bounds of this intersection should be

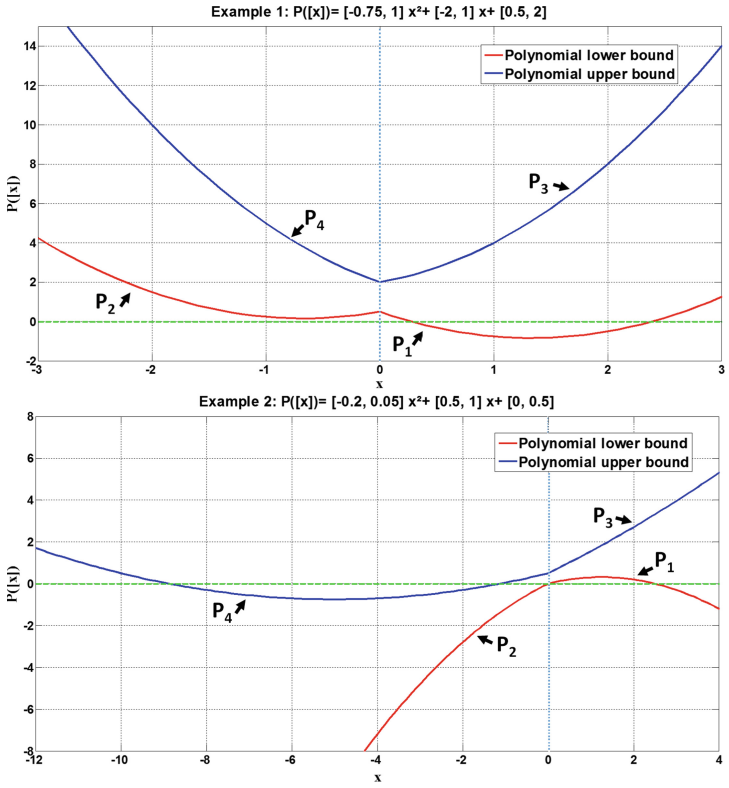

Fig. 2. Examples of interval polynomials [25].

accomplished by solving $P_{i=1..4}$. Once the roots of the boundary functions $P_{i=1..4}$ are calculated, it remains to clarify how to join these roots to formulate a precise enclosure of $P([x])$ solutions. Contrary to non-interval polynomials, $P([x])$ may have at maximum three distinct interval roots, including semi-infinite intervals (see Fig. 2).

In this paper, a simple algorithm is presented to extract $P([x])$ interval roots using $P_{i=1..4}$. It is based on the results obtained in [15] and [16], where the $P([x])$ coefficient bounds are analyzed to figure out the shape and orientation of $\underline{P}(x)$ and $\overline{P}(x)$. Consequently, the right number and values of the interval roots are appropriately determined. First, the number of sub-cases that must be checked to resolve $P([x])$ is decreased by admitting $\overline{a} > 0$. In the opposite case, the sign of $P([x])$ must be simply reversed. Therefore, each P_i must be solved by interval arithmetic. The readers must distinguish between solving interval polynomials and isolating real roots of standard polynomials. Several set-membership algorithms resolve the non-interval polynomials to bound rounding errors. In this work, the real roots of $P_{i=1..4}$ are computed numerically via an interval computation package. The isolated real roots associated to each P_i, including multiple

roots, are added to list L. Since functions P_1 and P_2 bound $P([x])$ only for $x \geq 0$ (see Eq. (15)), any negative root or part of a root must indefinitely be discarded from L. Seemingly, positive roots or parts of roots associated to P_3 and P_4 are dropped. Otherwise, there are some particular cases that must be considered while arranging L. Indeed, a double root is obtained at $x = 0$ for (P_1, P_2) when $\underline{c} = 0$ and respectively for (P_3, P_4) if $\overline{c} = 0$. For both cases, this root must be entered just one time to L. Besides, the infinite interval endpoints $\pm\infty$ must be placed if necessary in L. Referring to [15], once the following cases are satisfied, a lower endpoint $-\infty$ is added to L [25]:

$$\underline{a} < 0 \vee (\underline{a} = 0 \wedge \overline{b} > 0) \vee (\underline{a} = 0 \wedge \overline{b} = 0 \wedge \underline{c} \leq 0) \tag{17}$$

Likewise, $+\infty$ is added to L only if [25]:

$$\underline{a} < 0 \vee (\underline{a} = 0 \wedge \underline{b} > 0) \vee (\underline{a} = 0 \wedge \underline{b} = 0 \wedge \underline{c} \leq 0) \tag{18}$$

At this stage, L contains intervals that certainly present a lower or upper endpoint of the final interval roots of $P([x])$. Thus, it is necessary to recognize which are the lower and upper ones. Let denote $[S_i] = [\underline{S_i}, \overline{S_i}]$ the set of intervals held in L. All intervals $[S_i]$ are sorted such that $\underline{S_i} \leq \underline{S_{i+1}}$. It is worth mentioning that the adopted algorithm requires to consider $\pm\infty$ as degenerate intervals. Hence, n denotes the number of intervals included in L (no more than six roots $0 \leq n \leq 6$). The final step from the root finding strategy consists in arranging the solution according to the obtained n. Table 4 summarizes all probable shapes of the interval roots associated to $P([x])$. Finally, all necessary steps to solve the interval polynomial are recapitulated in Algorithm 1.

Table 4. Interval roots according to n [25].

	Interval roots
$n = 0$	$\varnothing$
$n = 2$	$[\underline{S_1}, \overline{S_2}]$
$n = 4$	$[\underline{S_1}, \overline{S_2}], [\underline{S_3}, \overline{S_4}]$
$n = 6$	$[-\infty, \overline{S_2}], [\underline{S_3}, \overline{S_4}], [\underline{S_5}, +\infty]$

6 Correlation-Based Optimization Step

In this work, the interval TTC formalizations are dedicated to ensure safety for an ACC. At every sample time, an enclosure for the position of target assigned to the ACC-equipped vehicle is defined proportionally to the $[TTC]$, which is calculated via the first or second-order model. Then, a reference distance d_{ref} is maintained from the in-front vehicle according to the worst-case risk indicated by the target enclosure (cf. Fig. 3).

Algorithm 1. Solving interval polynomial [25].

Require: $[a]$, $[b]$ and $[c]$.
Ensure : Solve $P([x]) = [a]x^2 + [b]x + [c]$.

1 -*Define* $P_{i=1..4}$ *(cf. equations (14) and (15)).*
2 -*Find interval roots of* $P_{i=1..4}$.
3 -*Put results in* L.
4 -*Add infinite entries* $\pm\infty$ *to* L*, if needed (cf. equations (17) and (18)).*
5 -*Sort the interval elements in* L *(*$\underline{S_i} \leq \underline{S_{i+1}}$*).*
6 -*Check the length of* L *to define roots of* $P([x])$.

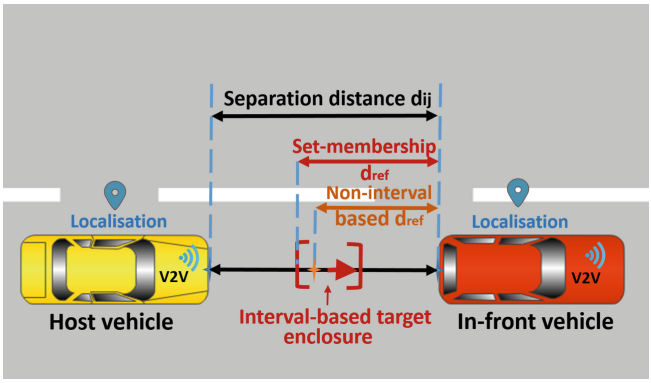

Fig. 3. Proposed ACC risk management principle [25].

Nevertheless, the interval over-approximations obtained via assumptions defined in Sect. 3 are too conservative. The occurrence of the worst cases of uncertainties for all parameters considered in the TTC computation is unrealistic. The ACC main task is to optimize the distance between vehicles to prevent congestion and traffic disturbances. Thus, the proposed method must make a trade off between safety and accuracy. In this context, a data-driven optimization step was introduced in [4,23] and [24]. Accordingly, this approach is joined to the TTC second-order model for more compact findings. In this section, this proposed data-driven approach is briefly recalled.

The main idea behind the proposed data-driven-optimization step is to examine the correlation progression over time. During the navigation run-time, substantial and brutal changes in vehicle dynamics are unrealistic in few sampling periods. Based on this understanding, the evolution of the correlation states should be smooth. Only uncertainties and erroneous measurements may invoke an irregular progression of correlation. Various data-driven approaches have relied on this assumption to capture faults or to regress outliers [7,42]. Uncertainties assigned to interval measurements can be over-estimated. This fact may entail a brutal variation in the correlation progression between two successive instants: t_{k-1} and t_k. Hence, the proposed approach narrows recursively intervals

until obtaining an acceptable progression in the correlation between variables. Narrowing is interpreted once the correlation relating the new tightened intervals matches reference values characterized off-line. Let denote by $C_{([X],[Y])|k}$ the correlation relating interval variables $[X]$ and $[Y]$ at instant t_k. The overall process to estimate the correlation for intervals variables is detailed in [23]. Thereafter, the gap in the correlation between instants t_k and t_{k-1}, denoted $\gamma_{k|k-1}$, is estimated through [25]:

$$\gamma_{k|k-1} = C_{([X],[Y])|k} - C_{([X],[Y])|k-1} \tag{19}$$

Interval widths must be narrowed in a recursive way to adapt the value of $\gamma_{k|k-1}$ in run-time and eliminate over-estimated uncertainties. For each couple of interval-valued variables intervening in the TTC computation, the interval with the largest width is concerned with iterative narrowing. After that, narrowing is aborted at two conditions:

- **Condition 1:** When $\gamma_{k|k-1}$ decreases from one iteration to another and suddenly starts to raise; i.e., the interval is narrowed as much as possible. Extra-narrowing may cause an undesirable modification in the correlation structure.
- **Condition 2:** Once $\gamma_{k|k-1}$ exceeds the minimum variation of correlation, which is recorded during the off-line simulation of a normal system operation.

Algorithm 2. [TTC] optimized estimation [25].

Inputs : p_i, p_j, V_i, V_j, $d_{i,j}$,$[T_{V2V}]$ and $[T_L]$.
Outputs: $[TTC_1]$ and $[TTC_2]$.

```
while Navigation process is running do
    -Define [d_{i,j}], [ḋ_{ij}], [d̈_{ij}], [V_i], [p_i] and [p_j].
    for each couple of variables between instants t_k and t_{k-1} do
        repeat
            -Calculate C_{([X],[Y])|k}.
            -Estimate γ_{k|k-1} (equation (19)).
            -Narrow the interval, if needed.
        until Condition 1 or 2 is satisfied
    end
    -Evaluate [TTC_1] and [TTC_2] (see equations (12) and (13))
end
```

7 Simulation Results

In this section, the reliability of the proposed interval-based models to compute the TTC is demonstrated. The quantitative results obtained from the conducted simulation are analyzed to provide a qualitative comparison between the performances of the first-order and second-order TTC formalizations.

7.1 Test Scenario and Simulation Setups

The overall set-membership TTC-based risk management is tested under a MATLAB freeway navigation simulator. Vehicle motions implicated in the test phase are simulated through the well-known tricycle kinematic model. The elaborated test scenario consists of a car-following scenario in a highway road. In addition, a model of a highway-road segment is selected as the test-scene. Otherwise, a white Gaussian noise is injected in the exact measurements of the navigation dynamics during simulation.

As already said, the follower vehicle is equipped with an ACC system. This latter exploits bounds of the interval TTC (according to the first or second-order model) to take precaution of the risk worst cases and adapt the reference distance from the vehicle ahead. Full details about the ACC operation principle are available in [24]. From a technical point of view, the interval computation is proceeded via the numerical computation package INTLAB (INTerval LABoratory). This latter is a chosen to play as an interval-based computation environment due to its high portability with MATLAB. In addition, INTLAB is selected to conduct the interval-based simulations due to its provable performances, rigorous results and fast computation [36].

All the simulation work depicted in this section is carried out under MATLAB on an Intel $i5$ Processor with 3.5 GHz and 16 GB memory. More configurations involved in the established simulation are recapitulated in Table 5.

Table 5. Simulation setups [25].

Parameter	Value
Sampling step	0.1 (s)
Leader maximum velocity	22 (m/s)
Follower maximum velocity	23 (m/s)

7.2 Quantification of Intra/Inter-vehicular Communication Delays

First of all, the V2V communication is assumed to be carried out through a DSRC tool. In that respect, a function that describes the behavior of the intra-vehicular latency is derived based on a simple interpolation applied on the experimental results illustrated in Tables 2 and 3. During the simulation run-time, the evolution of the V2V communication latencies is dynamically evaluated through the derived function. This behavior is directly involved in the results of different TTC formalizations suggested in this work.

The simulation considers also the potential margins of the intra-vehicular delays. In order to obtain a more realistic simulation environment, a model of the in-vehicular communication middleware based on the CAN protocol is integrated into the ACC system. Henceforth, it is possible to apply the CAN

dedicated-RTA model. As already stated, the different components from the end-to-end transmission time of the message which is responsible of delivering all the required data from the proposed AAC system sensing and communication layer to the risk management task to calculate the TTC. Indeed, Eq. (10) is used to assess the worst case of this message transmission time. The maximum blocking time entailed by the interferences between this message and the rest of messages initiated from the ACC operational blocks is defined based on a specific schedule. This latter is drawn during the development of the ACC model according to each message cruciality. For the local response times, all the involved measurement and sensing tools are assumed to have an up-date time of $0.01(s)$. The simulated electronic unit that performs the TTC-based risk management has a maximum execution time of $0.02s$ when the first order TTC formalization is used. This parameter is equal to $0.08s$ in the case of running the second-order set-membership TTC-based safety verification strategy. The RTA results as well as all the required details to compute the maximum transmission time of the data propagation through the on-board embedded system are delivered in Table 6.

Table 6. Communication setups and maximum latency results.

Parameter/result	Maximum value
CAN bit rate	500 Kbit/s
lm^{CAN}	5 Bytes
Interference blocking time	0.05 s
Message transmission time	0.21 ms
Risk management execution time (first order TTC)	0.02 s
Risk management execution time (second order TTC)	0.09 s
Message response time (first order TTC)	82.1 ms
Message response time (second order TTC)	150,21 ms

Thanks to the results of Table 6, it is simple to fix a relevant value of T_L according to a reasonable methodological manner.

7.3 Simulation Results and Discussion

At first, the role of the correlation analysis in providing more sharp bounds of TTC values is inspected. As shown in Fig. 4, the TTC enclosures are efficiently narrowed for both $[TTC_1]$ and $[TTC_2]$. For the first-order set-membership formalization, initial amounts of uncertainties are minimized with an average range of 60.3%. Similarly, the average reduction in the width of $[TTC_2]$ due to the correlation-based optimization step is about 65.79%.

More importantly, the results of the interval high-order TTC computation model are more conservative than the low-order one. In average, the widths of $[TTC_1]$ and $[TTC_2]$ are respectively about 1.25 s and 1.579 s. This fact can

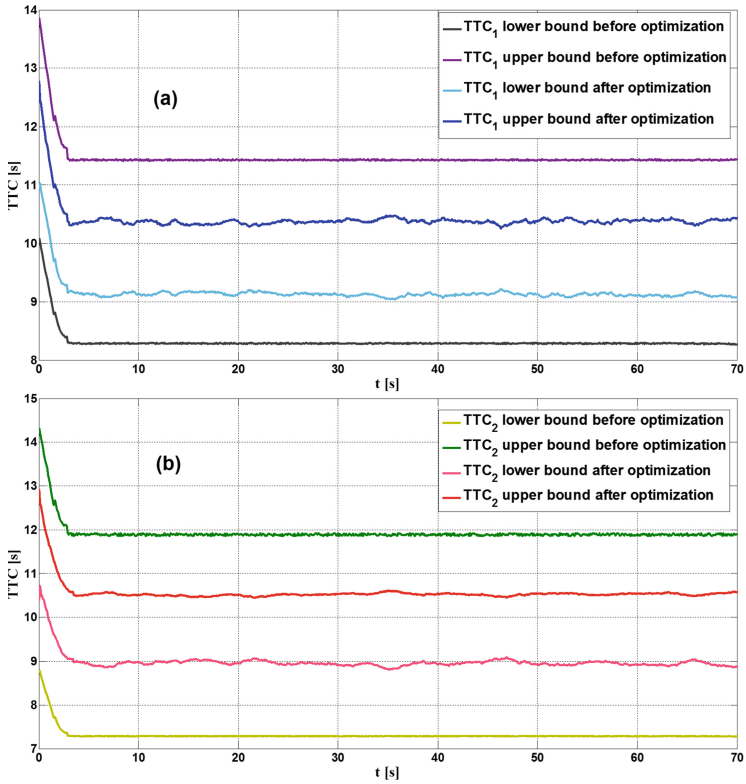

Fig. 4. TTC_1 and TTC_2 enclosures with/without optimization step [25].

be explained by the "dependency effect" characterizing the interval arithmetic [30]. Indeed, variables occurring several times in one expression are assumed as independently varying over their enclosures, which may lead to an additional pessimism in the results. Hence, more pessimism is entailed by upgrading the first-order-model to a second-order formalization since the number of the involved variables is increased.

In a second place, Fig. 5 illustrates the evolution of the exact TTC_1 and TTC_2. These exact values of TTC_1 and TTC_2 are obtained in a deterministic way (respectively via Eqs. (4) and (5)) without any noise injection during the simulation. All along the simulation run-time, the results of the two developed interval-based formalizations of the TTC enclose perfectly the reference values provided by the exact evolution of TTC_1 and TTC_2. Correspondingly, the consistency of the set-membership modeling joined with the correlation analysis is proven. Even more, the first-order interval-based TTC is more accurate than the second-one since it provides sharp bounds and simultaneously encompasses the exact and real values of the TTC. This fact optimizes implicitly the navigation traffic flow because it decreases the reference distance maintained between

vehicles. Eventually, the interval-based uncertainty quantification method contributes to compensate the inaccuracy presented by the first-order TTC resulting from the modeling simplification.

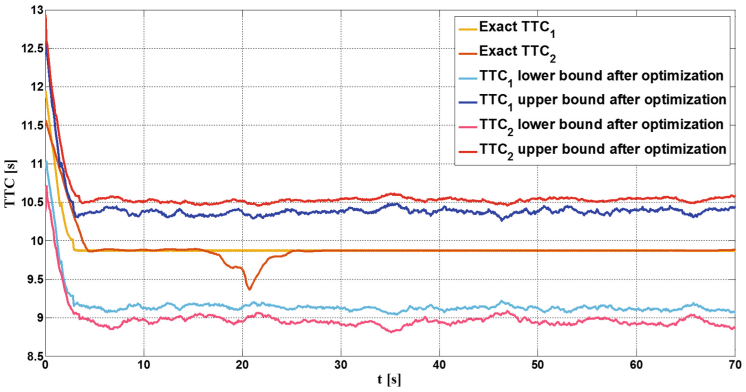

Fig. 5. TTC_1 and TTC_2 enclosures compared with exact results [25].

Another advantage of the proposed approach is the reduction in the computational cost of the risk management of intelligent vehicles. Using simple models, which handle efficiently all possible uncertainties, helps to respect the real-time constraints. In our case of study, solving the interval quadratic polynomial to compute an over-approximation to the TTC requires 0.06 s as an average execution time. Therefore, the TTC_1 is more efficient as a risk indicator than the TTC_2 especially in terms of computational demands. Additionally, the accuracy-level ensured by the TTC_1 is sufficient to guarantee the navigation safety since it handles properly uncertainties and modeling errors.

8 Conclusion

This work presents guaranteed solutions to handle uncertainties and risks endangering ITSs during car-following situations. As an approach to meet a safe and reliable autonomous navigation in the car-following context, a novel set-membership strategy to assess situational risk through the TTC computation is introduced. This new concept of the set-membership TTC combines the best features of the interval-based modeling of uncertainty evolution and the data-driven/correlation-based analysis of the system historical properties. Unlike the existing risk management and uncertainty handling methods, the defined strategy to quantify uncertainties and errors in the navigation dynamics relies on a careful consideration of sever new emergent challenges such as V2V communication latencies and automotive embedded system delays. The performances of the proposed models are compared. The results of the first-order TTC are more

compact and permit handling efficiently all uncertainties. Fast risk analysis with the same accuracy level of the second-order TTC is ensured via the simple low-order model. A tradeoff between accuracy and simplicity is ensured by joining the interval-based computation with correlation analysis. Accordingly, the need for sophisticated models for intelligent vehicles' motions to make the risk management successful is discarded, while mastering all uncertainty-induced risks. The carried out simulations demonstrated the proposed approach capabilities in ensuring safety, robustness against uncertainty and satisfying requirements of optimal navigation.

Otherwise, the proposed method should be integrated in the future on a real vehicle and applied for more critical maneuvers such as lane changes.

Acknowledgements. The present work is supported by the WOW (Wide Open to the World) program of the CAP 20-25 project. It receives also the support of IMobS3 Laboratory of Excellence (ANR-10-LABX-16-01).

References

1. Abdi, L., Meddeb, A.: Driver information system: a combination of augmented reality, deep learning and vehicular ad-hoc networks. Multimedia Tools Appl. **77**(12), 14673–14703 (2018). https://doi.org/10.1007/s11042-017-5054-6
2. Ahiska, K., Ozgoren, M.K., Leblebicioglu, M.K.: Autopilot design for vehicle cornering through icy roads. IEEE Trans. Veh. Technol. **67**(3), 1867–1880 (2018)
3. Aksjonov, A., Nedoma, P., Vodovozov, V., Petlenkov, E., Herrmann, M.: Detection and evaluation of driver distraction using machine learning and fuzzy logic. IEEE Trans. Intell. Transp. Syst. **20**(6), 2048–2059 (2019)
4. Ben Lakhel, N.M., Nasri, O., Gueddi, I., Ben Hadj Slama, J.: SDK decentralized diagnosis with vertices principle component analysis. In: 2016 International Conference on Control, Decision and Information Technologies (CoDIT), pp. 517–522 (2016)
5. Bock, F., Siegl, S., Bazan, P., Buchholz, P., German, R.: Reliability and test effort analysis of multi-sensor driver assistance systems. J. Syst. Architect. **85–86**, 1–13 (2018)
6. Chen, L., et al.: Survey of pedestrian action recognition techniques for autonomous driving. Tsinghua Sci. Technol. **25**(4), 458–470 (2020)
7. Chen, L., Yang, X., Liu, P.X., Li, C.: A novel outlier immune multipath fingerprinting model for indoor single-site localization. IEEE Access **7**, 21971–21980 (2019)
8. Cvjetkovic, M., Rakocevic, V.: Relative localisation algorithm for neighbour classification in ad hoc networks of moving robots. In: Proceedings of the First ACM International Workshop on the Engineering of Reliable, Robust, and Secure Embedded Wireless Sensing Systems, New York, NY, USA, pp. 46–53 (2017)
9. Dey, K.C., Rayamajhi, A., Chowdhury, M., Bhavsar, P., Martin, J.: Vehicle-to-vehicle (V2V) and vehicle-to-infrastructure (V2I) communication in a heterogeneous wireless network - performance evaluation. Transp. Res. Part C: Emerg. Technol. **68**, 168–184 (2016)
10. Durisic, D., Nilsson, M., Staron, M., Hansson, J.: Measuring the impact of changes to the complexity and coupling properties of automotive software systems. J. Syst. Softw. **86**(5), 1275–1293 (2013)

11. Fan, X., Deng, J., Chen, F.: Zeros of univariate interval polynomials. J. Comput. Appl. Math. **216**(2), 563–573 (2008)
12. Ferreira, J., Patrıcio, F., Oliveira, F.: A priori estimates for the zeros of interval polynomials. J. Comput. Appl. Math. **136**(1), 271–281 (2001)
13. Gamal, I., et al.: A robust, real-time and calibration-free lane departure warning system. Microprocess. Microsyst. **71**, 102874 (2019)
14. Gao, X., Su, D.: Suppression of a certain vehicle electrical field and magnetic field radiation resonance point. In: 2016 IEEE Vehicle Power and Propulsion Conference (VPPC), pp. 1–6 (2016)
15. Hansen, E., Walster, G.W.: Global Optimization Using Interval Analysis: Revised and Expanded, vol. 264. CRC Press, Boca Raton (2003)
16. Hansen, E.R., Walster, G.W.: Sharp bounds on interval polynomial roots. Reliable Comput. **8**(2), 115–122 (2002)
17. Hou, J., List, G.F., Guo, X.: New algorithms for computing the time-to-collision in freeway traffic simulation models. Comput. Intell. Neurosci. **2014**, 1–8 (2014)
18. Iberraken, D., Adouane, L., Denis, D.: Multi-level Bayesian decision-making for safe and flexible autonomous navigation in highway environment. In: 2018 IEEE/RSJ International Conference on Intelligent Robots and Systems (IROS), pp. 3984–3990 (2018)
19. Iberraken, D., Adouane, L., Denis, D.: Reliable risk management for autonomous vehicles based on sequential Bayesian decision networks and dynamic inter-vehicular assessment. In: IEEE 2019 IEEE Intelligent Vehicles Symposium (IV 2019), Paris-France, 9–12 June 2019
20. Jaulin, L., Kieffer, M., Didrit, O., Walter, E.: Applied Interval Analysis with Examples in Parameter and State Estimation, Robust Control and Robotics. Springer, London (2001). https://doi.org/10.1007/978-1-4471-0249-6
21. Khelifi, A., Ben Lakhal, N.M., Gharsallaoui, H., Nasri, O.: Artificial neural network-based fault detection. In: 2018 5th International Conference on Control, Decision and Information Technologies (CoDIT), pp. 1017–1022 (2018)
22. Lakhal, N.M.B., Adouane, L., Nasri, O., Slama, J.B.H.: Interval-based solutions for reliable and safe navigation of intelligent autonomous vehicles. In: 2019 12th International Workshop on Robot Motion and Control (RoMoCo), Poznań, Poland, pp. 124–130, July 2019. https://doi.org/10.1109/RoMoCo.2019.8787343
23. Lakhal, N.M.B., Adouane, L., Nasri, O., Slama, J.B.H.: Interval-based/data-driven risk management for intelligent vehicles: application to an adaptive cruise control system. In: 2019 IEEE Intelligent Vehicles Symposium (IV), Paris, France, pp. 239–244, June 2019. https://doi.org/10.1109/IVS.2019.8814216
24. Lakhal, N.M.B., Adouane, L., Nasri, O., Slama, J.B.H.: Risk management for intelligent vehicles based on interval analysis of TTC. IFAC-PapersOnLine **52**(8), 338–343 (2019). 10th IFAC Symposium on Intelligent Autonomous Vehicles IAV 2019
25. Lakhal., N.M.B., Nasri., O., Adouane., L., Slama., J.B.H.: Reliable modeling for safe navigation of intelligent vehicles: analysis of first and second order set-membership TTC. In: Proceedings of the 17th International Conference on Informatics in Control, Automation and Robotics - Volume 1: ICINCO, pp. 545–552. INSTICC, SciTePress (2020)
26. Lange, R., de Oliveira, R.S., Vasques, F.: A reference model for the timing analysis of heterogeneous automotive networks. Comput. Stand. Interfaces **45**, 13–25 (2016)
27. Lee, H., Ra, M., Kim, W.: Nighttime data augmentation using GAN for improving blind-spot detection. IEEE Access **8**, 48049–48059 (2020)

28. Lozenguez, G., Adouane, L., Beynier, A., Martinet, P., Mouaddib, A.I.: Map partitioning to approximate an exploration strategy in mobile robotics. In: Demazeau, Y., Pěchouček, M., Corchado, J.M., Pérez, J.B. (eds.) Advances on Practical Applications of Agents and Multiagent Systems. Advances in Intelligent and Soft Computing, vol. 88. Springer, Heidelberg (2011). https://doi.org/10.1007/978-3-642-19875-5_8
29. Makridis, M., Mattas, K., Ciuffo, B.: Response time and time headway of an adaptive cruise control. an empirical characterization and potential impacts on road capacity. IEEE Trans. Intell. Transp. Syst. **21**(4), 1677–1686 (2020)
30. Moore, R., Kearfott, R., Cloud, M.: Introduction to Interval Analysis. Society for Industrial and Applied Mathematics, Philadelphia (2009)
31. Nasri, O., Lakhal, N.M.B., Adouane, L., Slama, J.B.H.: Automotive decentralized diagnosis based on can real-time analysis. J. Syst. Architect. **98**, 249–258 (2019). https://doi.org/10.1016/j.sysarc.2019.01.009
32. Nicola, J., Jaulin, L.: Comparison of Kalman and interval approaches for the simultaneous localization and mapping of an underwater vehicle. In: Jaulin, L., et al. (eds.) Marine Robotics and Applications. OEO, vol. 10, pp. 117–136. Springer, Cham (2018). https://doi.org/10.1007/978-3-319-70724-2_8
33. Park, J., Abdel-Aty, M., Wu, Y., Mattei, I.: Enhancing in-vehicle driving assistance information under connected vehicle environment. IEEE Trans. Intell. Transp. Syst. **20**(9), 3558–3567 (2019)
34. Quaglia, D., Muradore, R.: Communication-aware bandwidth-optimized predictive control of motor drives in electric vehicles. IEEE Trans. Industr. Electron. **63**(9), 5602–5611 (2016)
35. Rigatos, G.G.: Nonlinear Kalman filters and particle filters for integrated navigation of unmanned aerial vehicles. Robot. Auton. Syst. **60**(7), 978–995 (2012)
36. Rump, S.: INTLAB - INTerval LABoratory. In: Csendes, T. (ed.) Developments in Reliable Computing, pp. 77–104. Kluwer Academic Publishers, Dordrecht (1999)
37. Tabernik, D., Skočaj, D.: Deep learning for large-scale traffic-sign detection and recognition. IEEE Trans. Intell. Transp. Syst. **21**(4), 1427–1440 (2020)
38. Talal, M., Ramli, K.N., Zaidan, A., Zaidan, B., Jumaa, F.: Review on car-following sensor based and data-generation mapping for safety and traffic management and road map toward ITS. Veh. Commun. **25**, 100280 (2020)
39. Vogt, P., Lenz, E., Klug, A., Westerfeld, H., Konigorski, U.: Robust two-degree-of-freedom wheel slip controller structure for anti-lock braking. IFAC-PapersOnLine **52**(5), 431–437 (2019). 9th IFAC Symposium on Advances in Automotive Control AAC 2019
40. Wang, S., Wang, W., Chen, B., Tse, C.K.: Convergence analysis of nonlinear Kalman filters with novel innovation-based method. Neurocomputing **289**, 188–194 (2018)
41. Ward, J.R., Agamennoni, G., Worrall, S., Bender, A., Nebot, E.: Extending time to collision for probabilistic reasoning in general traffic scenarios. Transp. Res. Part C: Emerg. Technol. **51**, 66–82 (2015)
42. Xia, B., Shang, Y., Nguyen, T., Mi, C.: A correlation based fault detection method for short circuits in battery packs. J. Power Sources **337**, 1–10 (2017)
43. Xie, G., Zeng, G., Liu, L., Li, R., Li, K.: High performance real-time scheduling of multiple mixed-criticality functions in heterogeneous distributed embedded systems. J. Syst. Architect. **70**, 3–14 (2016)
44. Yang, W., Wan, B., Qu, X.: A forward collision warning system using driving intention recognition of the front vehicle and V2V communication. IEEE Access **8**, 11268–11278 (2020)

45. Zhang, M., Deng, J.: Number of zeros of interval polynomials. J. Comput. Appl. Math. **237**(1), 102–110 (2013)
46. Zhang, W., Zheng, Y., Gao, Q., Mi, Z.: Part-aware region proposal for vehicle detection in high occlusion environment. IEEE Access **7**, 100383–100393 (2019)
47. Zhu, X., Zhang, H., Wang, J., Fang, Z.: Robust lateral motion control of electric ground vehicles with random network-induced delays. IEEE Trans. Veh. Technol. **64**(11), 4985–4995 (2015)